[*Nature* **313**, 293 (1985)] postulated that hydrous silicates could have been produced by reaction with unfrozen water on carbonaceous chondrite parent bodies. Calorimetric experiments demonstrate that carbonaceous chondrites can host unfrozen water [J. L. Gooding, *Lunar Planet. Sci. Conf.* **XV**, 228 (1984)].

16. S. B. Jones and D. Or, *Water Res. Res.* **35**, 929 (1999); Y. Taitel and L. Witte, *Chem. Eng. Sci.* **51**, 695 (1996).
17. D. W. G. Sears, H. W. Kochan, W. F. Huebner, *Meteorit. Planet. Sci.* **34**, 497 (1999).
18. E. D. Young and S. S. Russell, *Science* **282**, 452 (1998); S. S. Russell, L. A. Leshin, K. D. McKeegan, G. J. Macpherson, *Meteorit. Planet. Sci.* **32**, A88 (1997); S. Sahijpal, K. D. McKeegan, A. N. Krot, D. Weber, A. A. Ulyanov, *Meteorit. Planet. Sci.*, **34**, A101 (1999).
19. Magnetites precipitated from oxidation of Fe in an aqueous environment should have $\delta^{18}O$ values near that of water or several per mil lower than water on a mass fractionation curve. Equilibrium oxygen isotope fractionation between magnetite and liquid H_2O ($\delta^{18}O$ magnetite $-$ $\delta^{18}O$ H_2O) at 273 K is -0.1 per mil [Y. Zheng, *Geochim. Cosmochim. Acta* **55**, 2299 (1991)]. At the maximum temperatures that apply in our model ($\leq$323 K) the equilibrium $\delta^{18}O$ value for magnetite is 5 per mil lower than the $\delta^{18}O$ of coexisting H_2O. Magnetites from various chondrite groups lie on or near the slope 1.00 array or several per mil to the left of the array (lower $\delta^{18}O$) [B. Choi, K. D. McKeegan, A. N. Krot, J. T. Wasson, *Nature* **392**, 577 (1998); M. W. Rowe, R. N. Clayton, T. K. Mayeda, *Geochim. Cosmochim. Acta* **58**, 5341 (1994)], which is consistent with what is expected, based on the initial equilibrium partitioning between magnetite and water on the slope 1.00 line.
20. Bulk porosities of carbonaceous chondrite groups range from 10 to 30% by volume [L. Wilson, K. Keil, S. J. Love, *Meteorit. Planet. Sci.* **34**, 479 (1999)].
21. The initial $\delta^{17}O$ and $\delta^{18}O$ values for the water ice used in the model presented in this report are 2 and 3 per mil, respectively. Using initial values of 20 and 30 per mil for the water, as suggested by R. N. Clayton and T. K. Mayeda [*Earth Planet. Sci. Lett.* **67**, 151 (1984)], results in no appreciable change in our results downstream of the front, whereas the isotopic compositions of the phyllosilicate and carbonate minerals upstream of the front are similar to those in Fig. 3 but are displaced by approximately $+4$ per mil in $\delta^{18}O$ and $+3$ per mil in $\delta^{17}O$, resulting in a somewhat poorer fit to the CM and CI data.
22. Conventional fluorination data are from R. N. Clayton and T. K. Mayeda [*Earth Planet. Sci. Lett.* **67**, 151 (1984)] and from M. W. Rowe, R. N. Clayton, and T. K. Mayeda [*Geochim. Cosmochim. Acta* **58**, 5341 (1994)]. Secondary ion mass spectrometry analyses of Murchison CM carbonate were reported by A. J. Brearley, J. M. Saxton, I. C. Lyon, and G. Turner [*Lunar Planet. Sci. Conf.* **XXX**, CD-ROM (1999)].
23. Supported by a grant from the Particle Physics and Astronomy Research Council (PPA/G/S/1998/00069) of the United Kingdom.

3 August 1999; accepted 14 October 1999

Imaging of Humic Substance Macromolecular Structures in Water and Soils

S. C. B. Myneni,[1,3]* J. T. Brown,[2] G. A. Martinez,[4] W. Meyer-Ilse[2]

Humic substances (HSs) are the natural organic polyelectrolytes formed from the biochemical weathering of plant and animal remains. Their macromolecular structure and chemistry determine their role in biogeochemical processes. In situ spectromicroscopic evidence showed that the HS macromolecular structures (size and shape) vary as a function of HS origin (soil versus fluvial), solution chemistry, and the associated mineralogy. The HSs do not simply form coils in acidic or strong electrolyte solutions and elongated structures in dilute alkaline solutions. The macromolecular structural changes of HSs are likely to modify contaminant solubility, biotransformation, and the carbon cycle in soils and sediments.

Aqueous humic substances (HSs) exist primarily as soluble ions at low concentration and form colloids and precipitates at high concentration and when they react with cations and protons (*1, 2*). These changes can alter the HS macromolecular structures and subsequently affect the chemistry of HS coatings on mineral and colloid surfaces, the stability of organomineral aggregates, and the retention of pollutants and C in soils and sediments (*3–5*). Hence, direct information on the magnitude of changes in HS macromolecular structures, as a function of solution and substrate mineral chemistry, and their origin is critical for understanding the geochemical reactions mediated by natural organic molecules (*6*).

To test the influence of these parameters on natural organic molecule configuration, we conducted experiments on humic and fulvic acids isolated from river water (Suwannee River, Georgia), peat (Belle Glade, Florida), and soil (Mollic Epipedon, Illinois) samples. Fulvic and humic acid samples were the HS fractions isolated at alkaline and acidic pH, respectively, by the International Humic Substance Society and have been previously characterized (*7, 8*). The solution compositions tested were pH (2 to 12, adjusted with HCl or NaOH), ionic strength (0.01 to 2 M NaCl or 0.01 to 2 M $CaCl_2$), HS concentration (0.03 to 10 g of C liter^{-1}), and counterion composition (1 mM Cu^{2+} or Fe^{3+}). The influence of substrate mineralogy was examined for goethite (α-FeOOH), calcite ($CaCO_3$), and clays (kaolinite and montmorillonite), which are common to several soils and sediments (*9*). To correlate the macromolecular structures of isolated HSs with those of undisturbed natural samples, we also examined soil organic molecules in their pristine stage (organic molecules not extracted from surrounding soil matrix) for an Ultisol (Aquic Tropohumult, Puerto Rico) and an Alfisol (Kesterson Reservoir, California). These soils formed under contrasting chemical conditions with pH values of 5 and 8.0, respectively, and an organic C concentration of 1.5 and 0.3%, respectively. The macromolecular structures of HSs under these chemical conditions were examined directly at the high-resolution spectromicroscopy facility at the Advanced Light Source [Lawrence Berkeley National Laboratory (LBNL)] (*10*). The sample images were collected at the following x-ray photon energies: in the water window (516.6 eV) and at the Fe L (697 and 706 eV) and Cu L (933 and 936 eV) absorption edges. The contrast in images collected at the water window is dominated by the mass absorption of C and N atoms in the sample and helps in the determination of HS macromolecular structures. The images at the Fe and Cu edges, together with those obtained at the water window, are useful for examining cation and mineral association with HSs.

We examined the Suwannee River fulvic acid isolates with an x-ray microscope and found that they did not exhibit any measurable structures below a HS concentration of 1.0 g of C liter^{-1}. As the concentration was increased above 1.3 g of C liter^{-1}, HSs formed aggregates of different shapes and sizes (Fig. 1). In dilute, acidic, high-ionic-strength NaCl solutions, HSs predominantly formed globular aggregates and ringlike structures (Fig. 1A). As the fulvic acid concentration was increased, large sheetlike structures also formed and enclosed these smaller structures. Visible coiling was uncommon, and the HSs dispersed completely into aggregates of small size ($<$0.1 μm) in solutions of pH $>$ 8.0 (Fig. 1B). Although the addition of 1 M NaCl did not favor coiling under these alkaline conditions, concentrated HS solutions formed globular aggregates bound together with thin films of HSs. Additions of di- and trivalent cations to HS solutions promoted their precipitation at low C concentration and displayed macromolecular structures different from those formed in the presence of monovalent ions. In dilute fulvic acid solutions of Ca^{2+}, Cu^{2+}, or Fe^{3+}, the fulvic acids formed thin thread- and netlike structures (Fig. 1, C and D). As the fulvic acid and cation concentrations increased, these structures grew larger and formed rings and sheets (see Web fig. 1, available at www.sciencemag.org/feature/data/1043547.shl).

[1]Earth Sciences Division, [2]Center for X-ray Optics, Lawrence Berkeley National Laboratory, Berkeley, CA 94720, USA. [3]Department of Geosciences, Princeton University, Princeton, NJ 08544, USA. [4]Agriculture Experimental Station, University of Puerto Rico, Rio Piedras, PR 00928, USA.

*To whom correspondence should be addressed. E-mail: smyneni@princeton.edu

In contrast with the fluvial humics, the low solubility of soil and peat HSs promoted their precipitation at a much lower HS concentration than the fluvial isolates (~ 0.25 g of C liter^{-1} for soil fulvic acid in acidic NaCl solutions and at a lower concentration for humic acids and HSs in the presence of complexing cations). Although similar macromolecular structures were noticed for fluvial and soil HSs below a pH of 8.0, the latter arranged preferentially in globular and rod- or threadlike structures in dilute solutions (< 0.4 g of C liter^{-1}) and in sheetlike structures [occasionally with open holes (see Web fig. 2, available at www.sciencemag.org/feature/data/1043547.shl)] in concentrated solutions. In alkaline solutions, like their fluvial analogs, soil HSs also dispersed at low HS concentration and formed globular and sheetlike structures in concentrated solutions.

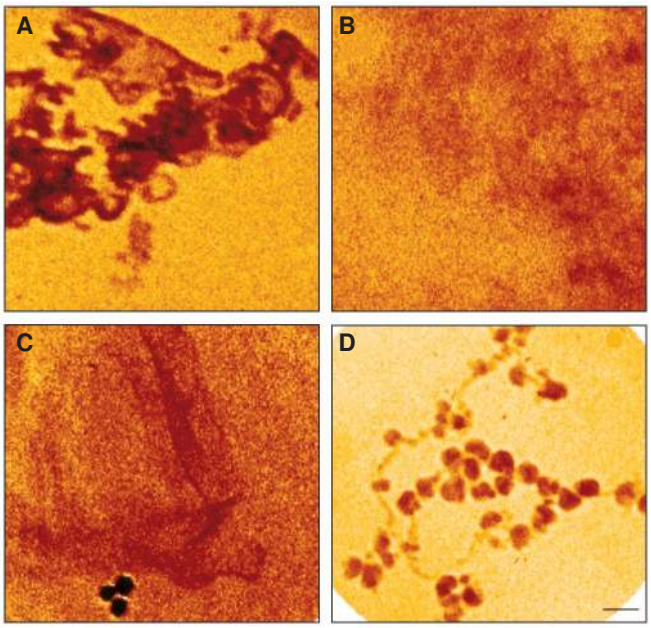

Fig. 1. Influence of pH, ionic strength, and complexing cations on the macromolecular structures of isolated fluvial fulvic acid. (**A**) pH is 3.0 ± 1.0, NaCl is 1.0 M, and C is ~1.5 g liter^{-1}. The average sizes of globular and ringlike structures were 0.3 μm (range of 0.2 to 0.45 μm) and 0.65 μm (range of 0.3 to 1.2 μm), respectively. The ratio of globular to ring structures was 70:30. In addition, sheetlike structures (average of 3 μm, range of 2 to 8 μm) were also noticed in concentrated HS solutions. (**B**) pH is 9.0 ± 1.0, NaCl is 0.5 M, and C is ~1.2 to 1.5 g liter^{-1}. Average aggregate size is <0.1 μm, with little deviation in size. In concentrated HS solutions, globular (average of 0.3 μm, range of 0.2 to 0.5 μm) and sheetlike structures (average of 1.5 μm, range of 1 to 5 μm) were also formed. (**C**) pH is ~4.0 ± 1.0, $CaCl_2$ is 0.018 M, and C is ~1.0 g liter^{-1}. The threadlike structures had an average length of ~3 μm (range of 2 to 6 μm) and a width of <0.15 μm. (**D**) pH is ~4.0 ± 1.0, Fe^{3+} is 1 mM, and C is ~0.1 g liter^{-1}. The average sizes of globular and threadlike structures were 0.3 μm (range of 0.25 to 0.4 μm) and 0.8 μm (range of 0.5 to 1.3 μm), respectively. Scale bar, 500 nm.

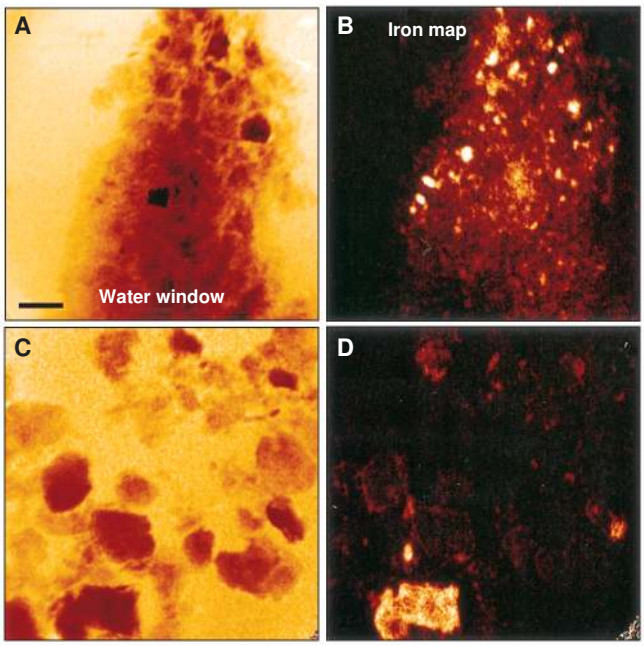

Fig. 2. Macromolecular structures of organic molecules in pine Ultisol. (**A** and **C**) Images collected at the water window. (**B** and **D**) Images collected at the Fe absorption edge. The brighter portions in the Fe map indicate particles rich in Fe. The ambient soil solution pH in (A) and (B) is 5.0. In (C) and (D), pH is 9.5 and NaCl is 1.0 M.

The presence of minerals completely altered the HS macromolecular structures in aqueous solutions. At low HS concentration (less than the aqueous saturation), sorption of HSs was evident by the formation of thin coatings on the mineral surfaces; these coatings could only be identified with the surface-sensitive photoemission spectromicroscopy methods. In saturated soil HS solutions of pH 2 to 10, clay minerals, goethite, and fine-sized calcite formed organomineral aggregates with thick HS coatings, which occurred as cement between mineral grains (Web fig. 2). Although the soil humic and fulvic acids displayed the same types of aggregate structures with minerals in alkaline solutions (pH > 8.0), soil humic acids predominantly formed aggregates that were less dense, mineral poor, and organic rich in the pH range of 2 to 7. As the HS concentration was increased well above its aqueous saturation, HSs formed thick coatings around minerals, irrespective of their composition. In addition to these organomineral structures, all of the mineral samples (except those in dilute HS solutions) also exhibited separate HS aggregates without any minerals, in globular and sheetlike forms. Although fluvial HSs showed similar behavior with mineral matrices, detectable organomineral aggregates formed at high HS concentration (>1.5 g of C liter^{-1}) only. Unlike soil HSs, fluvial fulvic and humic acids did not exhibit variation among their organomineral aggregate structures.

Humic substances not extracted from their surrounding soil matrices exhibited structures similar to those of isolated soil HS-mineral aggregates, as a function of HS concentration and pH. The pine Ultisol with high organic C content and low pH showed >100-nm-thick layers of organics on soil minerals, whereas the Alfisol with low C content, high pH, and high amount of dissolved salts showed thin organic coatings on minerals. Additions of salt solutions and increases in pH did not modify the organomineral aggregate structures in the pine Ultisol, but their size decreased notably at pH > 8.5 (Fig. 2, C and D). This resiliency of organomineral complexes is surprising because Fe oxides (and other common soil minerals) and humics bear a negative charge at those pH values and result in the dispersion of HS-mineral complexes exposing bare Fe oxide surfaces (*11*). These results indicate that the mineral surface chemistry plays a minor role in determining the HS macromolecular structures at high HS concentration. The similarities between the macromolecular structures of organomineral complexes in soils and those of isolates suggest that the results obtained from the latter can be applied to understand the behavior of HSs in soils and sediments.

We conclude that the type and concentration of HSs (fluvial versus soil) and electrolytes, pH, and mineral phases determine the macromolecular structures of humic materials. The changes

in HS macromolecular structures associated with solution chemistry may be caused by the protonation, deprotonation, and metal complexation of HS functional groups. The noted differences between the macromolecular structures of HSs of different origin are a reflection of the low solubility, higher aromatic C content, and the low carboxyl content of soil materials relative to fluvial humics (*1–6*). These results indicate that HSs exhibit more than one type of macromolecular structure in aqueous solutions, as opposed to the notion that HSs form rings in acidic and high ionic strength solutions and elongated structures in alkaline solutions (*12*). Globular and net-, ring-, and sheetlike structures have also been reported for soil HSs on substrate surfaces, such as mica and electron microscope sample substrates (*13–18*). As shown in this study, macromolecular structures of HSs associated with mineral oxides may not necessarily represent those in solution.

Changes in the HS macromolecular structures can modify the exposed surface area and alter the functional group chemistry of HSs, such as protonation and cation complexation. The common occurrence of HSs in more than one type of structure under pH conditions typical to the natural systems can substantially affect the biogeochemical processes in soils and sediments and the properties of aquatic colloids (*1–5*). In acidic soils and sediments with high C content, HSs can form dense structures with a low ratio of surface area to volume, in comparison to that of the alkaline soils. These structures can restrict the accessibility of micropores of HS aggregates to microorganisms and oxygen diffusion and thus inhibit the oxidation of organic matter and facilitate the stabilization of organic C by soils (*3–5*). Although fresh organic matter inputs are typically low in alkaline soils worldwide, the occurrence of HSs as open structures with high surface area under these conditions may also aggravate the C retention by alkaline soils (*4, 19*). For the same reasons, differences in HS macromolecular structures can also modify the intensity and rates of sorption, desorption, and biotransformation of contaminants (such as pesticides and chlorinated solvents) in soils and sediments (*3, 5*). Differences in the macromolecular structures of mineral-complexed HSs (with respect to size and C content) affect the properties of organomineral aggregates and control the chemistry of C retained by minerals in a soil profile, thus influencing the soil and sediment solution chemistry and their biogeochemical processes. These chemical and structural interactions of HSs can be explored directly with the high-resolution in situ x-ray spectromicroscopy methods.

References and Notes

1. F. J. Stevenson, *Humus Chemistry* (Wiley, New York, 1994).
2. D. S. Orlov, *Humic Substances of Soils and General Theory of Humification* (Balkema, Brookfield, VT, 1995).
3. R. Schwarzenbach, P. M. Gschwend, D. M. Imboden, *Environmental Organic Chemistry* (Wiley, New York, 1993).
4. J. I. Hedges and J. M. Oades, *Org. Geochem.* **27**, 319 (1997).
5. P. M. Huang and M. Schnitzer, *Soil Sci. Soc. Am. Spec. Publ. 17* (1986).
6. M. Schnitzer, *Soil Sci.* **151**, 41 (1991).
7. R. C. Averett, J. A. Leenheer, D. M. McKnight, K. A. Thorn, *U.S. Geol. Surv. Water Supply Pap. 2373* (1995).
8. D. L. Spark, Ed., *Methods of Soil Analysis: Part 3, Chemical Methods* (Soil Science Society of America, Madison, WI, 1996).
9. Kaolinite and montmorillonite were obtained from the Clay Mineral Society, calcite was reagent grade, and goethite was prepared by titrating $FeCl_3$ solution. The solid concentration in the experiments varied between 1 and 5 g of mineral per liter.
10. In an x-ray microscope, the contrast of the sample comes from the photoelectric absorption of x-rays, and hence, element- and functional group–specific images can be obtained at high spectral resolution for organic molecules. This instrument uses zone-plate optics to illuminate the sample (~10-μm field) and to form an enlarged image on an x-ray charge-coupled device camera. The spatial resolution of the microscope is currently 43 nm, limited by the zone-plate optics. However, the Poisson noise slightly reduces the resolution for images taken above the oxygen K-edge (543 eV) because of absorption by water. In addition, the sample nature (for example, mineral versus microbe) also determines the attainable spatial resolution. For collecting images, liquid samples or soil pastes (5.0 μl) were placed between two Si_3N_4 windows (thickness, 100 nm), and this entire assembly was placed at the focal point of the zone plates. Small changes in the concentration of soluble species may occur in samples because of water evaporation losses during imaging. To prevent such changes, we collected images immediately after they were placed in the holder. The chemical conditions reported here represent samples in the initial stages. Typically, the x-ray exposure to the sample varied from a few seconds to 60 s. The natural organics did not show any visible damage or modifications under these exposure times or after several exposures. For more information on the x-ray microscope of LBNL, see work by W. Meyer-Ilse *et al.*, *Synchrotron Radiat. News* **8**, 29 (1995). Descriptions of x-ray spectromicroscopy are available in work by G. Schmahl *et al.*, *Optik* **93**, 95 (1993); J. Kirz, C. Jacobson, M. Howells, *Q. Rev. Biophys.* **28**, 33 (1995); and J. Thieme *et al.*, *X-ray Microscopy and Spectromicroscopy* (Springer, Berlin, 1998).
11. W. Stumm, *Chemistry of the Solid-Water Interfaces* (Wiley, New York, 1993).
12. K. Ghosh and M. Schnitzer, *Soil Sci.* **129**, 266 (1980).
13. Y. Chen and M. Schnitzer, *Soil Sci. Soc. Am. J.* **40**, 682 (1976).
14. I. L. Stevenson and M. Schnitzer, *Soil Sci.* **133**, 179 (1982).
15. J. Buffle *et al.*, *Environ. Sci. Technol.* **32**, 2887 (1998).
16. N. Senesi, F. R. Rizzi, P. Acquafredda, *Colloids Surf A* **127**, 57 (1997).
17. D. K. Namjesnik and P. A. Maurice, *Colloids Surf. A* **120**, 77 (1997).
18. P. A. Maurice and D. K. Namjesnik, *Environ. Sci. Technol.* **33**, 1538 (1999).
19. H. Jenny, *Factors of Soil Formation: A System of Quantitative Pedology* (McGraw-Hill, New York, 1941).

20. S.C.B.M. dedicates this paper in memory of his co-author, Werner Meyer-Ilse. The authors thank T. K. Tokunaga, S. M. Benson, G. E. Brown, G. Sposito, S. J. Traina, and P. Maurice for helpful discussions and reviews of the manuscript and A. Lucero for help with the image processing. The research is funded by the Laboratory Directed Research and Development program of LBNL and by the Basic Energy Sciences (Geosciences) program of the U.S. Department of Energy.

14 July 1999; accepted 12 October 1999

Origin of Magnetization Decay in Spin-Dependent Tunnel Junctions

Martha R. McCartney,[1]* Rafal E. Dunin-Borkowski,[1]† Michael R. Scheinfein,[2] David J. Smith,[1,2] Savas Gider,[3] Stuart S. P. Parkin[3]

Spin-dependent tunnel junctions based on magnetically hard and soft ferromagnetic layers separated by a thin insulating barrier have emerged as prime candidates for information storage. However, the observed instability of the magnetically hard reference layer, leading to magnetization decay during field cycling of the adjacent soft layer, is a serious concern for future device applications. Using Lorentz electron microscopy and micromagnetic simulations, the hard-layer decay was found to result from large fringing fields surrounding magnetic domain walls in the magnetically soft layer. The formation and motion of these walls causes statistical flipping of magnetic moments in randomly oriented grains of the hard layer, with a progressive trend toward disorder and eventual demagnetization.

The resurgence of interest in magnetic thin films has been driven by the discovery of large magnetoresistance (MR) effects in multilayered films (*1*–3), spin-valve structures (*4*), and tunnel junctions (*5*, *6*). Typically, spin-dependent magnetic tunnel junctions (MTJs) consist of ferromagnetic (FM) layers separated by a thin insulating barrier, which is most often alumina. When the magnetization directions of the FM layers are parallel, there is a high probability of electrons with like spins tunneling between layers, and the resistance (R) is low. Conversely, when the magnetization is antiparallel, the tunneling probability is low and R is high. Devices based on the MR effect, such as magnetic